Development of a real time rock characterization system using drilling dynamics simulator - application to horizonal well operation technology

Mejbahul Sarker

Abstract - Despite recent advances in drilling operation risk and safety, downhole tools damage and wellbore instabilities are still the leading causes of major problems in oilwell drilling operations. Improving safety and optimum design of drilling operation requires good and reliable rock characterization. Although such characterization can be possible with the instantaneous drilling data acquisition system but without having an appropriate data processing tool, i.e. a drilling simulator, some of the information will become invaluable and has motivated extensive research on development of an improved computer-based drilling simulator. This paper offers a brief review of the drilling rock characterization methods, followed by introduction and discussion of the rock characterization methods by developed computer-based drilling simulator. The simulator includes a dynamic model for 3D motions of a BHA with wellbore stick-slip whirl interaction and combines the model with a model of the drill pipe and collars. The pipe and collars are modeled using a lumped-segment approach that predicts axial and torsional vibrations. The simulator can predict how axial and torsional bit-rock reaction are propagated to the surface, and the role that lateral vibrations near the bit play in exciting those vibrations and stressing components in the BHA. The proposed simulator includes the mutual dependence of these vibrations, which arises due to bit-rock interaction and friction dynamics between the drillstring and wellbore wall. Finally, the simulator has been used to drill a horizontal well in simulation using the parameters used in the field. The simulator has been tuned to reproduce field drilling behavior and used to investigate different drilling scenarios with the objective of finding most desirable conditions for drilling a future well in a similar geological well. A brief overview of the results of the preliminary study and initial observation on a drilling simulator and summary of the suggested improvements are also discussed.

Keyword: Drilling, rock characterization, computer-based simulator, bottom-hole-assembly, dynamic motions, bond graph, simulation.

1. Introduction

Rock drilling optimization has acquired greater significance due to increase in less familiar rock zones and to greater depths. Since the early twentieth century there are very few published field case studies that have reported problem free drilling operations. Field experience shows that mud motor, drill bit, measurement while drilling (MWD), and BHA component failures are very common during drilling operations. Especially during extended-reach lateral wells drilling that maximizes reservoir contact, which are much more complex than standard horizontal wells, the failure cause time-consuming and costly trips out of the hole. Downhole data shows that vibration in the BHA is one of the main reasons for these failures. To overcome the failures, identification the sources of the vibrations and adjusting the drilling parameters to eliminate the vibrations are required for successful drilling operations. One of the important factors of concern to the engineers in the general field of rock drilling is to assess the physico-mechanical properties of rock. Whereas drill bits responses are extremely sensitive to formation properties and operating conditions. Early detection of formation changes and appropriate adjustment of the operational variables are important measures to execute optimal well plan and drilling performance. The more that is known about rock formation, the better it can be optimized. A computer-based drilling simulator is very important to forecast the rock formations. Interest in establishing the computer-based drilling simulator is mainly motivated by the need to improve the interpretation of drilling vibrations for rock characterization and drilling optimization. The interaction of drill bit with rocks is one of the major excitation source of drilling vibrations due to the percussion and cutting action of the bit. The induced axial vibrations at the bit can lead to lateral vibrations in the bottom hole assembly (BHA), and axial and torsional vibrations observed at the rig floor may be related to severe lateral vibrations downhole near the bit. The severity of these vibrations depends on the formation properties as well the drilling operation itself. Thus, measurements of the drill bit vibrations can be a tool to predict formation properties. Investigation of rock properties based on drilling performance measurements have been carried out by many researchers. Kahraman *et al.* [1] presented a penetration rate model for rotary blast hole drills using the drillability index. The model was validated for the formations having uniaxial compressive strength over 40 MPa and especially for carbonaceous rocks. The correlations between the drillability index and rock properties has been incorporated in the model to estimate the penetration rate of rotary blast hole drills. In another research, Kahraman [2]

investigated the correlations between the modulus ratio and penetration rate of rotary and percussive drills using the raw data obtained from the experimental works. The statistical model shows the penetration rates of percussive drills increases linearly with an increasing modulus ratio. However, the derived equations require to be validated for other rocks. Bilgin and Kahraman [3] further presented a correlation between the penetration rates and the rock properties and developed a regression equation. The plots show that the penetration rate strongly depends on the uniaxial compressive strength, the point load strength, schmidt hammer value, cerchar hardness and impact strength.

Hoseinie *et al.* [4] presented a study of rock properties affecting the penetration rate of pneumatic top hammer drills. The drilling rate of pneumatic top hammer drills was correlated with dry density, uniaxial compressive strength, tensile strength, Schmidt hammer rebound number, Young's modulus, mean hardness, mean grain size, equivalent quarts content and Schimazek's F-abrasivity of nine rocks. The rock samples were drilled using an actual pneumatic top hammer drilling machine with a 3 ½ inch diameter cross type bit. The results showed that the tensile strength, uniaxial compressive strength and Schmidt hammer rebound affects the drilling rate. The analysis did not consider the effect of drilling parameters and bit diameter on the drilling rate.

Nygaard and Hareland [5] developed a methodology to estimate drilling time and bit wear before drilling using the rock strength data. Logs, rock mechanical tests and drilling data have been used to measure the rock strength. The predictions of rock strength were verified and modified using the daily drilling data. The bit wear and rock strength were re-simulated based on the actual drilling conditions. The rock strength log from the reference well were slightly higher than the actual well but the correlation were fine. Also, the drilling time prognosed was same as the actual. The results show that strength logs can be a very valuable tool for developing drilling prognosis. And the quality of the prognosis was determined on the lithological homogeneity and on the availability of data for constructing the rock strength log. In another research, Hareland and Nygaard [6] utilized the drilling data in calculating rock strength, correlations were developed from inverted rate of penetration models. From these models unconfined compressive rock strength was calculated from drilling data. The rate of penetration models accounted operational drilling parameters, bit types/designs and geological formation information. Finally, the drilling-based rock strength estimation method was verified using data from various onshore and offshore fields. The results show that this method effectively predicted the rock strength.

Archer and Rasouli [7] used a log-based methodology to extract rock elastic and strength properties as well as the magnitude of stresses including vertical and maximum and minimum horizontal stresses. The methodology was based on the fundamental relationship between physical properties of rocks as captured in petrophysical logs (sound velocity or density) and mechanical properties (uniaxial compressive strength). The log-based analysis was applied to a shale gas well drilled in the North Perth Basin. The continuous logs of elastic and strength properties were calibrated at some depths where the triaxial lab tests results were reported on some core samples. The rock mechanical model was used as an input for hydraulic fracture initiation pressure and sanding analysis.

Amani and Shahbazi [8] calculated the uniaxial compressive strength (UCS) based on a sonic log as a function of sonic travel and formation porosity. A quantitative relationship was developed between the UCS and sonic travel time and formation porosity. Results show that well segment length has a notable impact on precision and extension of obtained. A theoretical work was done to make the most accurate relationship to predict UCS in carbonate in Ahwaz oil field. The developed 3D model was accurately predicted the UCS than obtained equation related to just transient time.

Tahmeen *et al.* [9] presented a convenient and cost-effective technology that uses drilling data to calculate the geomechanical properties. A well bore friction model and inverted ROP models were utilized to calculate the coefficient of friction, effective downhole weight on bit and rock geomechanical properties, respectively. The model was verified with downhole measurements form Copilot. The calculated geomechanical property logs generated from the proposed data-driven technology was further compared to actual laboratory determined rock properties.

Yenice [10] presented a drilling rate index (DRI) model based on UCS and Brazilian tensile strength (BTS) of rock. The relations between DRI and two geomechanical properties were established using simple and multiple regression analysis. Results show that the DRI has a strong relation with the UCS for the rocks with strength above 100 MPa.

Kalantari *et al.* [11] developed a theoretical model based on limit equilibrium of forces and considering contact frictions, crushed zone and bit geometry in the rotary drilling process. A developed portable drilling machine was used to drill the rocks with different strength and to record the operational drilling parameters such as thrust force, torque, rate of penetration and speed of rotation. The conducted drilling experiment used three different rocks ranged from weak, medium and hard strength. The UCS was calculated using cutting point method. The results show that the proposed model can effectively predict UCS, cohesion and internal friction angle of rock. However, the resulting torque and thrust from lower indentation rates were not well fitted to the results of the conventional standard tests.

Most of the studies reported that rock samples were collected from drilling locations and the physico-mechanical

properties were determined both in the field and the laboratory. During drilling in the site or laboratory, various drilling performance parameters were measured. These results were analyzed to develop best-fit correlation between the drilling parameters and rock properties. Although such characterization can be possible with the instantaneous drilling data acquisition system but without having an appropriate data processing tool, i.e. a drilling simulator, some of the information will become invaluable and has motivated extensive research on development of a computationally efficient yet predictive computer-based drilling simulator to understand the dynamic behavior of rock-bit and to predict the rock strength. This study addresses the relationships between the induced drillstring vibrations due to bit-rock interaction and rock strength.

This paper is organized as follows. Section 2 presents a review of drilling simulators software. Section 3 describes the proposed drilling dynamic simulator. A complete drilling dynamic simulator that allows to predict the effect of formation changes on drillstring responses is presented in Section 4. Conclusions are given in Section 5.

2. A review of drilling simulator

Drilling operations management faces hurdles to reduce costs and increase performance with less experience and organizational drilling capacity. Usually, the more that is known about a system, the better it can be controlled and optimized. Such knowledge can come from direct state measurement or from estimates of state, using some facsimile of the assemblage, or both. For a complicated system such as rotary rock drilling in which measurements are limited, a simulator is required not only to supplement the available measurements but to provide a basis for useful interpretation of the data. Such a simulator must meet certain criteria including adequate description of the system under most operating conditions. Where these conditions are highly variable or little known, the simulator should be of such a nature that it can be used adaptively. The simulator must be such that it can be utilized simply and quickly to achieve desired objectives. Different approaches have been made to develop drilling simulator software. Millheim and Huggins [12] developed an engineering simulator for drilling (ESD), an analytical system's approach to planning and analyzing drilling systems in real or faster than real time. The complex drilling system has been subdivided into component parts of geology, the drilling rig, wellbore, fluid system, and the drillstring. Each subsystem has been represented as a set of algorithms that best depict the physics of the system. The interaction between the algorithms has been considered to represent the complete drilling process. The ESD was designed specifically for the drilling person and limited to vertical well drilling application. In another research, Millheim [13] defined simulator as a device or piece of equipment that replicates some physical process or operation to some level of fidelity. The simulated has been related to the numerical or logical replication of some process, operation, or phenomenon. Millheim and Gaebler [14] further introduced the concept of the virtual experience of simulation. The introduced methods show how experience and knowledge gained in a certain domain, i.e. drilling a well, can be captured and retained, as well as being used as a tool to transfer learning. The developed simulator was based on the actual data of 22 wells drilled in a specific geographical and geological environment. The results obtained are in excellent agreement with the actual data in the field.

Cooper *et al.* [15] presented an interactive program for student or engineer to simulate the drilling of an oil well, and to optimize the drilling process by comparing different drilling plans. The simulator consisted three main parts, a lithology editor, a settings editor and the simulation program itself. The lithology editor allows the student, instructor or engineer to build a real or imaginary sequence of rock layers, each characterized by its mineralogy, drilling and log responses. Whereas the settings editor defines the operational parameters, ranging from the drilling and wear rates of bits in specific rocks to the costs of different procedures. Finally, the simulator contains an algorithm that determines rate of penetration and rate of wear of bit as drilling continues, and whether the well kicks or fractures, and assigns various other accident conditions. In another research, Cooper *et al.* [16] presented a simulator that allows drilling, logging, and other operations to be carried out so that the student gradually learns about the properties of the filed during a series of hands on exercise. Abouzeid and Cooper [17] further discussed the use of drilling simulator to help in the planning of future wells if information is available from offset wells. The proposed simulator software which is built using the drilling mechanics model can be readjusted to reproduce the drilling performance observed in the offset well.

Rampersad *et al.* [18] presented a geological drilling log (GDL) using drilling models specific to the bits used for individual intervals to generate a formation profile of properties for the entire section drilled on a foot by foot basis. The drilling models are capable of accurately simulating the drilling of a well and reproducing realistic rates of penetration. In another research, Bratli *et al.* [19] presented the drilling optimization simulator (DROPS) to reduce the cost of future wells based on GDL, created from the data collected in a previous well drilled in the same area. Whereas, the GDL is created using rate of penetration models inverted to calculate rock compressive strength. Hareland *et al.* [20] further discussed the use of apparent rock strength log (ARSL) in the drilling simulator. Using the data from the

reference well, an ARSL is generated by the inversion of the bit specific rate of penetration model. The effects of drilling hydraulics, mud rheology, and pore pressure are integral to the model. The follow-up phase involves a continuous evaluation of the drilling progress. During this phase updates are conducted to verify and, if needed, modify model predictions. Variations in operating parameters and lithology are continuously evaluated. The resulting effects on predicted performance and bit wear condition are determined and relayed back to the drilling location.

Dubinsky and Baecker [21] presented an interactive PC-based simulator to simulate the dynamic behavior of the drill bit for numerous downhole and surface factors, such as hook load, RPM, mud properties and flow rate, BHA configuration, drill bit design, borehole parameters, and formation properties. The system accurately simulated the major drilling dynamic dysfunctions, such as bit bounce, lateral vibrations, BHA/bit whirl, torque shocks, stick-slip and torsional oscillation. The basic tool for creating the simulator internal model incorporates the system identification approach. The simulator's program consists some quite complicated nonlinearities. However, the simulator's effectiveness depends upon the amount of data used for developing and training the model.

Booth *et al.* [22] discussed a prototype software drilling simulator that incorporates both wellbore stability and rate of penetration modules. The simulator allows drilling practices to be closely linked with geological models. It provides a framework which integrates previously stand-alone aspects of drilling planning and decision support. It uses visualization techniques to convey complex models and results simply.

Rommetveit *et al.* [23] presented an innovated system, called *eDrilling*, for real time drilling simulation, 3D visualization and control from a remote drilling expert centre. The system development concept uses all available real time drilling data (surface and downhole) in combination with real time modeling to monitor and optimize the drilling process. The system allows to visualize the wellbore in 3D in rea time. The system can provide important information on key drilling parameters like hydraulics profile, temperature profile, friction conditions along the drillstring and wellbore, cutting transport conditions, well instability tendencies, pore pressure ahead of drill bit, optimal ROP, all in real time. The system also makes automatic diagnosis of upcoming drilling problems by combining real time simulations with drilling data.

Ahmed *et al.* [24] presented a new approach to develop and apply drilling simulation systems by collaboration between industry and academia. A total of two drilling simulators has been proposed. One of the simulator concepts uses a physical drilling model that replicates hoisting, rotating, and circulating functions while drilling actual or simulated rock. The other simulatorconsists of modern drilling control equipment combined with advanced computer models of the drilling process. The computer models of the drilling process support standard drilling operations such as tripping in/out, stand building, and drilling itself, including a downhole model that takes into account the effects of rock porosity, pore pressure, unconfined strength, and internal friction angle on rate of penetration.

Vassillos *et al.* [25] described a drilling simulator that simulates the drilling process using WOB, RPM, flow, survey and lithology data and predicts ROP. The simulator is used to predict rock strength, find optimal rheological model from viscometer data, and optimize bit nozzle selection. It allows for fine tuning of the process. Overall, the simulator was able of simulating any formation types.

Existing research work shows that the virtual experience simulator, geological drilling logs, and reconstructed lithology are some of the most successful. The drilling simulations can run multiple scenarios quickly and then update plans with new data to improve the results. Its storage capacity for retaining field drilling experience and knowledge add value to the program. The paper presents a demonstration of deviated wellbore drilling dynamic simulator for predicting the vibrations and show the effect of rock formation on these vibrations. There is considerable literature that analyzes the dynamics of a vertical drillstring. Each author uses a different approach to model the drillstring dynamics: cosseral theory [25], one mode approximation [26], beam modes together with finite element method [27], and discretized systems with two degrees of freedom [28]. There are few papers treating the dynamic modeling of deviated drillstrings. In almost all the models describes in [29-30] only the BHA up to the so-called point of tangency is taken into account by the dynamic analysis, whereas the model in [31] includes continuous wall contact and the main focus was on the parametric excitation of lateral vibrations due to fluctuating weight on bit (WOB). Recently an analytical solution for the threshold rotary speed, after which the drillstring starts to snack, is derived and presented in [32]. Also, the analytical results are verified using a versatile finite element formulation to model the drillstring in greater detail. The above research work shows that no complete dynamic model for a directional oilwell drillstring, capturing axial, lateral, and torsional vibrations, has been developed. Therefore, development of a dynamic model of a directional oilwell drillstring that shows the mutual dependence of axial, torsional and lateral vibrations, which arise due to interactions of drill bit with the formation and drillstring with the borehole wall, has been focused in this paper.

3. Description of proposed drilling dynamic simulator

The proposed approach to the drilling simulator is less broad, focusing primarily on drilling dynamics. For the model development a unified modeling approach using bond graph method was employed as an alternative to traditional modeling and simulation techniques. The traditional modeling and simulation techniques for dynamic systems are generally adequate for single domain systems only. Whereas the development of an efficient yet predictive dynamic model for a deviated oilwell drillstring is extremely multidisciplinary, requiring knowledge of top drive motor dynamics, contact-friction phenomena in the curve and horizontal section, 3D BHA dynamics, hydrodynamic damping and bit-rock interaction phenomena. Bond graph method can offer a new modeling and simulation methodology that is ideally suited to effectively unify knowledge pertaining to multi domain systems for oilwell drilling applications. The graphical nature of bond graphs separates the system structure from the equations, making bond graphs ideal for visualizing the essential characteristics of a system. Indeed, by creating bond graphs, designing, and analyzing the structure of a system - perhaps the most important part of the modeling task – can offer be undertaken using only a pencil and paper. Modelers can thus focus on the relationships among components and subsystems rather than the implementation details of their modeling software. Even before a computer is used, bond graphs can provide an engineer with information about constrained states, algebraic loops, and the benefits and consequences of potential approximations and simplifications. Many computer-based modeling tools are available for generating and processing bond graphs. The 20-sim software [38] developed at the University of Twente (Netherlands) is based on the well-known block oriented TUTSIM simulation program and has been used in this paperwork. The tool has the capabilities that extend far beyond those of traditional block-diagram software, including generation of symbolic representations, model inversion, and parametric identification as well as the ability to produce simulations, frequency responses, and other design aids. An overview of bond graph approach is given in Appx A.

The system being modeled consists of drill pipes (DP), heavy weight drill pipes (HWDP), "subs" such as navigation and logging tools, collars, mud motors, the drill bit and the rock (formation). "Motor HS", which is run by drilling mud, rotates the drill bit with respect to the rest of the string. Drilling fluid is circulated in the drillstring and the annular space between the drillstring and the wellbore. The drilling fluid is characterized by the flow rate developed by the mud pumps. The top of the drillstring is subject to a tension force, applied through the surface cables. Rotary motion is applied by an armature controlled motor, through a gear box, to the rotary table via the Kelly (a square, hexagonal or octagonal tube that is inserted through and is an integral part of the rotary table that moves freely vertically while the rotary table turns it. The essential components of the horizontal drillstring are shown in Fig. 1. The whole drillstring modeling is divided into two sections. Section one includes the vertical portion, curved portion and major horizontal portion. The 56m long final horizontal portion ending at the bit is called section two.

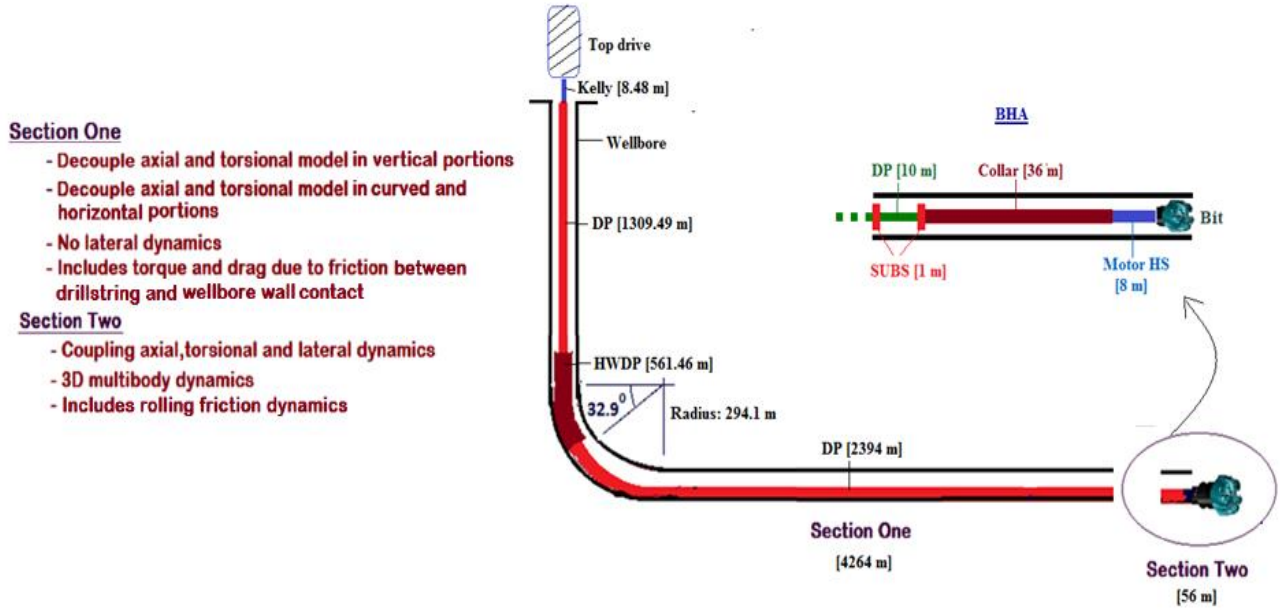

Figure 1: Schematic of the horizontal drillstring for modeling and simulation.

3.1 Modeling of top drive motor dynamics

Usually the top drive consists of one or more motors (electric and hydraulic) connected with appropriate gearing to a short section of pipe, which in turn may be screwed into the drillstring. In this paperwork a bond graph model for AC induction motor has been considered to simulate the top drive system. Fig.B1 presents the complete bond graph model of an induction motor based on its electrical equivalent circuit [39]. Four fluxes ($\lambda_{s\alpha}$, $\lambda_{r\alpha}$, $\lambda_{s\beta}$ and $\lambda_{r\beta}$) and the angular momentum of the rotor are used as the state variables. The proposed induction motor model has been driven by a three-phase fixed frequency balanced ac supply. Effort sources Se: V_a, Se: V_b, and Se: V_c having sinusoidal voltages with equal amplitude but with corresponding phase angles of 0, $-2\pi/3$, $2\pi/3$ phase angles, respectively, have been used to excite the system.

3.2 Modeling Section One

A lumped-segment approach is used in the axial and torsional dynamic model. In the lumped segment approach, the system is divided into a series of inertias, interconnected with springs [40-41]. The accuracy of the model natural frequencies depends on the number of elements considered, however, in contrast to a modal expansion approach [40], the analytical mode shapes and natural frequencies need not be determined. If a system model is divided into many elements, then the accuracy of the results will be very high compared to a low number of segments model. The behavior will approach that of a continuous system as the number of segments approaches infinity. The model accounts for the effect of drilling fluid circulation in the drillstring and the annular space between the drillstring and the wellbore, on drillstring motions. The drilling fluid was characterized by the flow rate developed by the mud pumps. Nonlaminar Newtonian flow formulations are used in calculation of fluid drag force/damping for the longitudinal motion. Hydrodynamic damping due to drilling fluid circulation in the drillstring and the annular space was considered in the longitudinal direction instead of viscous damping. In the case of torsional motion, the viscous damping which results from the contact between drillstring surfaces and the drilling fluid was considered. In addition, the model considers the self-weight effect and buoyancy effect due to drilling fluid. A bond graph model for the longitudinal and torsional motions of a vertical drillstring segment is shown in Fig. B2. The terms V_p and V_a in the figures indicate drilling mud velocity inside drillstring and the annulus, respectively. The reader is referred to [42] for the equations of the fluid drag forces and rotational fluid friction to the drillstring motions. The axial bond graph shows a mass (I element) and gravity force source (Se element) associated with segment velocity *v*. Hydrodynamic dissipative forces (R elements) also contribute to Newton's Second Law of the mass, with the flow sources (Sf) and 0-junctions calculating relative fluid flow velocities inside and outside the pipe. The dissipative forces are functions of these relative velocities. Axial compliance and material damping of the segment are modeled by parallel compliance (C) and dissipative elements, the forces of which are functions of the relative velocity (calculated by the 0-junction) of the segment with respect to the adjoining segment. The buoyancy weight of the drillstring segment acts in the longitudinal direction for the case of vertical drilling. It is not the same while drilling the build (or curved) section where a portion of buoyancy weight acts in the longitudinal direction and is shown in Fig. B3 as an effective weight. For the case of horizontal section drilling, there will be no contribution of buoyancy weight in the longitudinal direction. The curve and horizontal drillstring segment models have the friction terms (Fig. B3 and Fig. B4), whereas friction loss has been neglected in the vertical sections.

In the vertical portion, the contact between drillstring and wellbore wall is neglected. For curved and horizontal portions, the contact and friction between drillstring and wellbore wall are considered. Stick-slip is very common when the relative velocity the sliding surfaces approaches zero and the surface become 'stuck', requiring a force larger than the maximum static sliding friction force to break the surfaces loose. Karnopp [43] and Margolis [44] developed well-known bond graph models for stick-slip friction. Sarker *et al.* [45] presented a modified Margolis friction model and has been used in this paper. The friction elements (C elements) in the bond graph model shown in Fig. B3 and B4 provide drag force for longitudinal motion and transverse frictional force which multiplies with drillstring radius to provide frictional torque for torsional motion. The reader is referred to [45] for a complete development and validation of the bond graph models for Section One.

3.3 Modeling Section Two

The 56m long horizontal portion of the drillstring shown in Fig. 1 is modelled using a 3D multibody dynamics approach implemented in vector bond graphs. The multibody bond graph method facilitates connection of the pipe models to models of such elements as motors, bearings, shock absorbers, and in-line vibrators to simulate percussive drilling. Rigid lumped segments with 6 degrees of freedom are connected by axial, torsional, shear, and bending springs to approximate continuous system response. Parasitic springs and dampers are used to enforce boundary conditions. Accuracy increases with the number of lumped segments used. However, increasing the number of segments leads to larger simulation times and there is no closed-form relation between the number of segments in a model and accuracy of the natural frequencies or total response. Drillstring contact

with the wellbore wall, which can occur continuously over a line of contact for horizontal drillstrings, generates normal forces using a user-definable stiff spring constitutive law. Fig. B5 and B6 show the 3D multibody bond graph models segments for section Two of the drillstring. The reader is referred to [46] for more details on the 3D multibody bond graph modeling development and validation for Section Two.

Tangential contact forces due to friction between the drillstring and wellbore wall must be generated to whirl to occur. The potential for backward whirl, as seen in drilling applications, requires the transition from pipe-wellbore sliding motion to a motion where the pipe rolls without slip around the wellbore surface. The model computes the relative velocity between sliding surfaces when contact occurs and enforces a rolling-without-slip constraint as the velocity approaches zero. The bond graph model to capture the pure rolling and rolling with sliding is shown in Fig. B7. The modulated transformer (MTF) elements in Fig. B6 enforces the velocity constraints of the 'Whirl Speed' equation. The transformer (TF: Radius, r) converts pipe spin speed into tangential velocity. The (small) difference between tangential and whirl velocities is the velocity with which a virtual stiff spring (C) deforms during the stick phase. When the spring force exceeds the maximum available static friction force, the spring releases to allow slip. The "Mse:Fwb_A11" element computes and applies a normal contact force from the spring in Fig. B7 during a collision. The reader referred to [46] for more details on the stick-slip whirl interaction phenomena modeling for Section Two.

3.4 Modeling Bit-rock interaction

The bit-rock interaction provides coupling between axial and torsional drillstring dynamics. In this present work a quasi-static rock-bit model is used instead of a computationally intensive and difficult-to-parameterized complete dynamic representation. Yigit and Christoforou [26] have shown a static rock-bit interaction model in a drillstring represented using only two inertias and one compliance for both axial and torsional motions. Their model is modified as described below. The original model in [26] assumed both friction and cutting torque regardless of whether dynamic weight on bit was sufficient to create penetration and cuttings. Depth of cut was a function of average rather than instantaneous rotation speed, along with rate of penetration. Rate of penetration was a function of average rotation speed and a constant applied weight on bit (WOB), rather than dynamic weight on bit. This paper incorporates threshold force and the effect of instantaneous WOB and bit rotation speed on cutting torque on bit (TOB). Below a threshold force W_{fs}, the drill tool does not penetrate the rock, leaving only friction as a source of TOB. The bit-rock interaction model in [26] could not allow the drill bit to move longitudinally as the drill bit cut the rock formation. Thus, the bit-rock model has been modified accordingly. This has the important benefit of allowing prediction of ROP. The dynamic WOB equation has been modified as follows:

$$\mathrm{WOB} = \begin{cases} \mathrm{k}_c\left(x - s - \int ROP\right) & if\ x \geq (s + \int ROP) \\ 0 & if\ x < (s + \int ROP) \end{cases} \quad (1)$$

where k_c and s indicate formation contact stiffness and bottom-hole surface profile. Surface profile is given as:

$$\mathrm{s} = \mathrm{s}_0\, f(\emptyset) \quad (2)$$

The formation elevation function $f(\emptyset)$ is chosen to be sinusoidal, $f(\emptyset) = \sin b\emptyset$, where b indicates bit factor which depends on the bit type. The term $\emptyset$ indicates rotational displacement of the bit.

The total torque on bit (TOB) is related to frictional and cutting conditions, and dynamic WOB. When bit rotary speed is in the positive direction then TOB can be written as

$$\mathrm{TOB} = \begin{cases} \mathrm{TOB}_f + \mathrm{TOB}_C & WOB > \mathrm{W}_{fs} \\ \mathrm{TOB}_f & WOB \leq \mathrm{W}_{fs} \end{cases} \quad (3)$$

In the case of zero-bit rotary speed

$$\mathrm{TOB} = \begin{cases} \mathrm{TOB}_C & WOB > \mathrm{W}_{fs} \\ 0 & WOB \leq \mathrm{W}_{fs} \end{cases} \quad (4)$$

Finally, for negative bit rotary speed

$$\mathrm{TOB} = \mathrm{TOB}_f \quad (5)$$

where TOB_f and TOB_C represent frictional and cutting torque on bit and both are calculated as below,

$$\mathrm{TOB}_f = (\mathrm{WOB}) r_b \mu(\dot{\phi}) \tag{6}$$

$$\mathrm{TOB}_C = (\mathrm{WOB}) r_b \xi \sqrt{\frac{\delta_C}{r_b}} \tag{7}$$

The term $\dot{\phi}$ indicates instantaneous bit rotary speed, and the function $\mu(\dot{\phi})$ characterizes the friction process at the bit and it is given as

$$\mu(\dot{\phi}) = \mu_0 \left(\tanh \dot{\phi} + \frac{\alpha \dot{\phi}}{(1+\beta \dot{\phi}^{2\gamma})} + \nu \dot{\phi} \right) \tag{8}$$

where μ_0, α, β, γ, and ν are the experimentally determined parameters of the frictional model. In equation (7) the terms $r_b$and δ_C indicate bit radius and depth of cut per revolution, the latter given as

$$\delta_C = \frac{2\pi \mathrm{ROP}}{\dot{\phi}} \tag{9}$$

The instantaneous rate of penetration (ROP) is a function of dynamic WOB, instantaneous bit speed $\dot{\phi}$, and rock/bit characteristics. The modified ROP equation from [26] can be written as

$$\mathrm{ROP} = C_1 \mathrm{WOB} \sqrt{\dot{\phi}} + C_2 \tag{10}$$

where ξ, C_1 and C_2 characterize the cutting action at the bit and depend on the type of the bit and formation. The physical sketch of the contact between drill bit and rock formation is shown in Fig. 2, and the bond graph model is shown in Fig. 3.

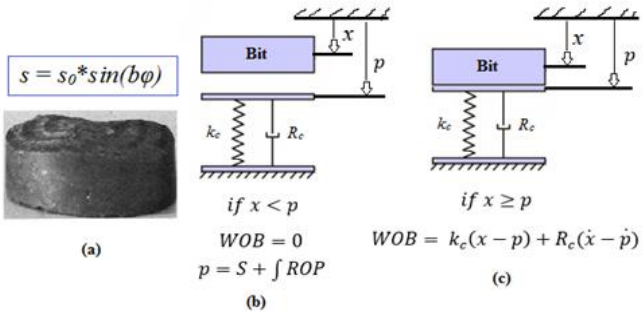

Figure 2: sketches show (a) a lobe pattern of formation surface elevation, and (b) bit and rock spring-damper representation when x < p and (c) bit contact with rock when x >= p rock spring and damper under compression.

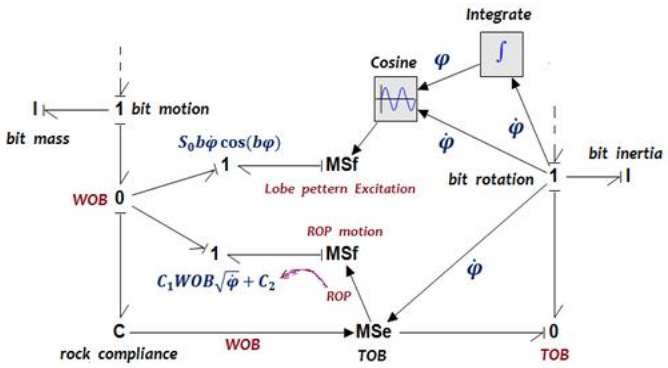

Figure 3: Bond graph model of bit-rock motion

4. Simulation results

The bond graph model of the horizontal drillstring has been developed in 20Sim®. The main objective of this simulation is to show the ability of the proposed simulator to capture the effect of rock property on drilling dynamic responses. The bit-rock interaction model has the capability to advance the bit and predict the ROP. Data from the actual well (Table C1) is used for simulation. The simulation results for a 4320 m total depth are shown in Figs. 4-8. The top of the drillstring is rotated at 10 rad/sec while the mud motor is rotated at 13.7 rad/sec (Figs. 4). Simulation results in Fig. 5 show that the drill bit rotates with high torsional oscillations and the average angular speed is the combined speed of the top drive and mud motor shown in Fig. 4. The surface torque required to overcome the cutting torque at the bit and frictional torque throughout the drilling is shown in Fig. 5. The unsteady WOB (Fig. 4) and bit speed provide an unsteady ROP that can be verified from ROP plot in Fig. 5.

The simulation has been carried out for considering the two rock formations (i.e. Hackensack Siltstone and Pierre Shale I) and the Table C2 summarizes the stiffness and damping values of these rocks. The first 40 seconds of simulation show the drilling results for Hackensack Siltstone and the rest of the results are for Pierre Shale I. The WOB plot in Fig. 4 indicates the severe axial vibrations due to the hard formation (i.e. Pierre Shale I) whereas the less axial vibration is found for the case of drilling the less hard formation (i.e. Hackensack Siltstone). The axial vibration results can be verified from dynamic force plots at behind the bit (Fig. 6). The forces at the behind bit show the similar trend found in the WOB plot. Also, the formation changes during drilling the soft to hard formation is verified from both the WOB plot and dynamic forces plot at the behind bit. The high axial contact dynamic force at the 40 sec simulation time indicates the transition between the soft to hard formation.

The bit speed plot in Fig. 5 shows the lower average rotations for the hard formation compared to the soft formation. The increased torque due to the drilling the hard formation is found to be the main reason for the lower bit rotations. The ROP plot in Fig. 5 clearly differentiate the formation types which show the lower penetration for the case of hard formation compared to the soft formation. The high oscillation in the ROP plot for the case of soft formation is found to be another way for differentiating the rock types. The drillstring whirling speed plots in Fig. 6 show the less fluctuations for the case of hard formation which is significantly found at 17 m behind the bit.

Fig. 7 shows the plots of the contact forces between the bottomhole assembly of the drillstring and wellbore formations. The continuous detachments between the drillstring and wellbore formation has been found for the case of drilling the soft formation whereas the continuous contact is dominant for the case of drilling the hard formation. Thus, the contact force measurement shows another effective way of characterizing the formation types. The horizontal well dynamic drilling simulator described herein is effective at predicting the effect of formation type changes on drilling responses. Determining the type of formations through simulation is a cost-effective way of developing a real time rock characterization software tool.

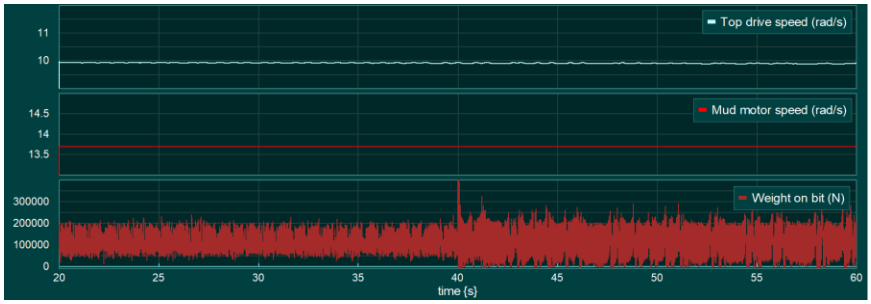

Figure 4: Top drive speed, mud motor speed and WOB plots of a horizontal drilling dynamic simulator.

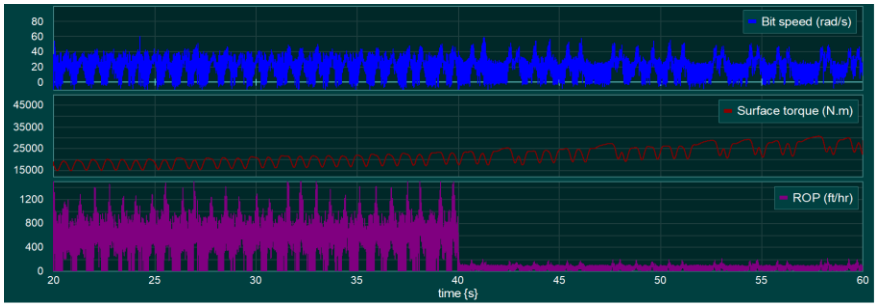

Figure 5: Bit speed, surface torque and ROP plots of a horizontal drilling dynamic simulator.

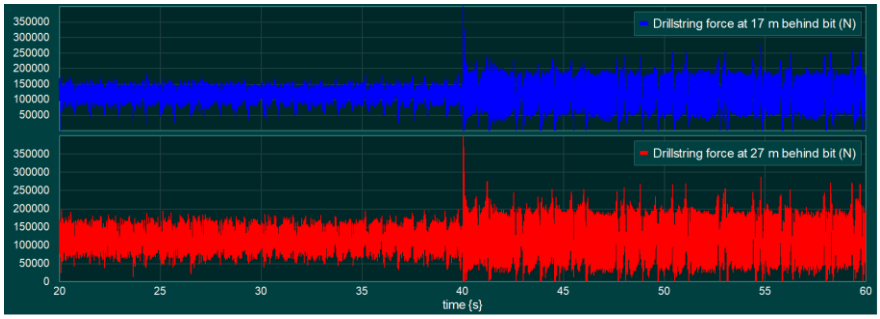

Figure 6: Force plots at 17m behind the bit and 27 m behind the bit of a horizontal drilling dynamic simulator.

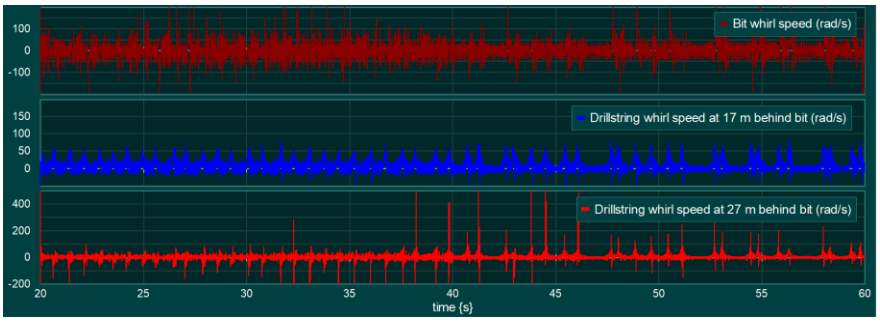

Figure 7: Whirl speed plots at the bit, 17 m behind the bit and 27 m behind the bit of a horizontal drilling dynamic simulator.

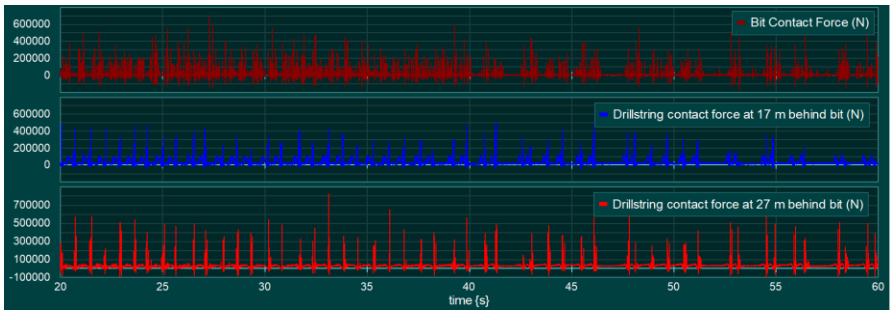

Figure 8: Contact force plots at the bit, 17 m behind the bit and 27 m behind the bit of a horizontal drilling dynamic simulator.

5. Conclusions

Application of a drilling dynamic simulator for simulating the formation types in a horizontal well has been presented. The drillstring bottom-hole-assembly has been modeled using a three-dimensional multibody dynamics approach implemented in vector bond graphs. Rigid lumped segments with 6 degrees of freedom are connected by axial, torsional, shear, and bending springs to approximate continuous system response. Parasitic springs and dampers are used to enforce boundary conditions. A complete deviated drillstring has been simulated by combining the bottom-hole-assembly model with a model of drill pipe and collars. The pipe and collars are modeled using a lumped-segment approach that predict axial and torsional motions. The model can predict how axial and torsional bit-rock reactions are propagated to the surface, and the role that lateral motions near the bit plays in exciting those motions, which arises due to bit-rock interaction and friction dynamics between drillstring and wellbore wall formation. The model effectively simulates the effect of rock types on drillstring dynamic responses. Simulation results show a better rock characterization is possible through analyzing the plots of drillstring dynamic responses. The uniqueness of this proposed work lies in developing an efficient yet predictive drilling dynamic simulator for characterization of rocks for a deviated well.

References

[1] Kahraman, S., Balci, C., Yazici, S. and Bilgin, N. (2000). Prediction of the penetration rate of rotary blasthole drilling using a new drill ability index. *International Journal of Rock Mechanics and Mining Science*, V. 37, 729-43.

[2] Kahraman, S. (2003). Performance analysis of drilling machines using rock modulus ratio. *The Journal of the South African Institute of Mining and Metallurgy*. 515-522.

[3] Kahraman, S. and Bilgin, N. (2003). Drillability prediction in rotary blast hole drilling. *International Mining Congress and Exhibition of Turkey – IMCET*, ISBN 975-395-605-3.

[4] Hoseinie, S.H., Ataei, M. and Aghababaie, A. (2014). A lab study of rock properties affecting the penetration rate of pneumatic top hammer drills. *Journal of Mining and Environment.* V.5(1), 25-34.

[5] Nygaard, R. and Hareland, G. (2007). Application of rock strength in drilling evaluation. Presented at the *SPE Latin American and Caribbean Petroleum Engineering Conference* in Buenos Aires, Argentina, 15-18 April.

[6] Hareland, G. and Nygaard, R. (2007). Calculating unconfine rock strength from drilling data. Presented at the *American Rock Mechanics Association*, *U.S. Rock Mechanics Symposium*, 27-31 May, Vancouver, Canada.

[7] Archer, S. and Rasouli, V. (2012). A log-based analysis to estimate mechanical properties and in-situ stresses in a shale gas well in North Perth Basin. *WIT Transactions on Engineering Science*.

[8] Amani, A. and Shahbazi, K. (2013). Prediction of rock strength using drilling data and sonic logs. *International Journal of Computer Applications*, Volume 81 – No2. 7-10.

[9] Tahmeen, M., Love, J., Rashidi, B. and Hareland, G. (2017). Complete geomechanical property log from drilling data in unconventional horizontal wells. Presented at the 51st *US Rock Mechanics/Geomechanics Symposium*, San Francisco, California, USA, 25-28 June.

[10] Yenice, H. (2019). Determination of drilling rate index based on rock strength using regression analysis. *An Acad Bras Cienc*. 91 (3).

[11] Kalantari, S., Hashemolhosseini, H. and Baghbanam, A. (2018). Estimating rock strength parameters using drilling data. *International Journal of Rock Mechanics and Mining Sciences*, V. 104, 45-52.

[12] Millheim, K.K. and Hussins, R.L. (1983). An engineering simulator for drilling: part I. *Presented at the Annual Technical Conference and Exhibition*, San Francisco, 5-8 October.

[13] Millheim, K.K. (1986). The role of the simulator in drilling operations. *SPE Drilling Engineering*, October, pp 347-357.

[14] Millheim, K.K. and Gaebler, T. (1999). Virtual experience simulation for drilling – the concept. Presented at the *SPE/IADC Drilling Conference*, Amsterdam, The Netherlands, 9-11 March.

[15] Cooper, G.A., Cooper, A.G. and Bihn, G. (1995). An interactive simulator for teaching and research. Presented at the *Petroleum Computer Conference*, Houston, 11-14 June.

[16] Cooper, G.A., Mota, J.F. and Cooper, A.G. (1996). Integrated petroleum engineering simulator and decision making teaching program. Presented at the *Annual Technical Conference and Exhibition*, Denver, 6 October.

[17] Abouzeid, A.A. and Cooper, G.A. (2001). The use of a drilling simulator to optimize a well drilling plan. Presented at the *Geothermal Resources Council Annual Meeting*, San Antonio, Texas, 26-29 August.

[18] Rampersad, P.R., Hareland, G. and Boonyapaluk, P. (1994). Drilling optimization using drilling data and available technology. Presented at the *SPE LAPEC Conference*, Buenos Aires, 27-29 April.

[19] Bratli, R.K., Hareland, G., Stene, G.W., Dunsaed, G.W. and Gjelstad, G. (1997). Drilling optimization software verified in the North Sea. Presented at the *SPE LACPEC Conference*, Rio de Janeiro, 30 August – 2 September.

[20] Hareland, G., Rampersand, P.R., and Skar, O.M. (2000). Simulation can help optimize drilling and cut cost. *Drilling Contractor*, No 6, 42.

[21] Dubinsky, V.S. and Baecker, D.R. (1998). An interactive drilling dynamics simulator for drilling optimization and training. Presented at the *SPE Annual Technical Conference and Exhibition*, New Orleans, Louisiana, 27-30 September.

[22] Booth, J., Bradford, I.D.R., Cook, J.M., Dowell, J.D., Ritchie, G. and Tuddenham, I. (2001). Meeting future drilling planning and decision support requirements: a new drilling simulator. Presented at the *SPE/IADC drilling conference*, Amsterdam, The Netherland, 27 February – 1 March.

[23] Rommetveit, R., Bjørkevoll, K.S., Ødegård, S.I., Herbert, M., Halsey, G.W., Kluge, R. and Korsvold, T. (2008). eDrilling used on Ekofisk for real-time drilling supervision, simulation, 3D Visualization and Diagnosis. Presented at the *SPE Intelligent Energy Conference and Exhibition*, Amsterdam, The Netherlands, 25-27 February.

[24] Ahmed, R.M., Smith, J.R., Bohorquez, V.B. and Koederitz, W.L. (2010). Novel applications of drilling simulators in student recruitment, teaching and research programs. Presented at the *IADC/SPE Drilling Conference and Exhibition*, New Orleans, Louisiana, USA, 2-4 February.

[25] Kelessidis, V.C., Ahmed, S. and Koulldis, A. (2015). An improved drilling simulator for operations, research and training. Presented at the *SPE Middle East Oil and Gas Show*, Manama, Bahrain, 8-11 March.

[25] Tucker, R.W. and Wang, C. (1999). An Integrated Model for Drill-string Dynamics. *Journal of Sound and Vibration*, 224(1), 123-165.

[26] Yigit, A.S. and Christoforou, A.P. (2006). Stick-slip and Bit-bounce Interaction in Oil-well Drillstrings. *Journal of Energy Resources Technology*, 128(4), 268-274.

[27] Khulief, Y.A., Al-Sulaiman, F.A. and Bashmal, S. (2007). Vibration Analysis of Drillstrings with Self-excited Stick-slip Oscillations. *Journal of Sound and Vibration*, 299(3), 540-558.

[28] Richard, T., Germay, C. and Detournay, E. (2004). Self-excited Stick-slip Oscillations of Drill bits. *Mecanique* 332, 619–626.

[29] Millheim, K.K. and Apostal, M.C. (1981). The Effect of Bottomhole Assembly Dynamics on the Trajectory of a Bit. *Journal of Petroleum Technology*, S. 2323-2338.

[30] Burgess, T.M., McDaniel, G.L. and Das, P.K. (1987). Improving BHA Tool Reliability with Drillstring Vibration Models: Field Experience and Limitations. *SPE/IADC Drilling Conference*, New Orleans, Louisiana, USA.

[31] Dunayevsky, V.A., Judzis, A. and Mills, W.H. (1985). Dynamic Stability of Drillstring under Fluctuating Weight-on-Bit. *Presented at the 60th Annual Technical Conference of the SPE*, Las Vegas, Nevada, USA.

[32] Heisig, G. and Neubert, M. (2000). Lateral Drillstring Vibration in Extended-Reach Wells. *SPE/IADC Drilling Conference*, New Orleans, Louisiana, USA.

[33] Sarker, M., Rideout, D.G. and Butt, S.D. (2012). Dynamic Model of an Oilwell Drillstring with Stick-slip and Bit-bounce Interaction. *10th International Conference on Bond Graph Modeling and Simulation*, Genoa, Italy.

[34] Sarker, M., Rideout, D.G., Butt, S.D., 2014. Dynamic modeling of horizontal shafts with annular surface contact and friction – application to oilwell drilling. In: Presented at *ASME International Mechanical Engineering Congress and Exposition*. Montreal, Quebec, Canada, November 14–20.

[35] Sarker, M., Rideout, D.G., Butt, S.D., 2016. Analysis of stick-slip friction between the drillstring and borehole wall in horizontal wells. In: *12th International Conference on Bond Graph Modeling and Simulation*. Montreal, Quebec, Canada, July 24–27.

[36] Sarker, M., Rideout, D.G., Butt, S.D., 2017. Dynamic model for longitudinal and torsional motions of a horizontal oilwell drillstring with wellbore stick-slip friction. *J. Petrol. Sci. Eng.* 150, 272–287.

[37] Sarker, M., Rideout, D.G., Butt, S.D., 2017. Dynamic model for 3D motions of a horizontal oilwell BHA with wellbore stick-slip whirl interaction. *J. Petrol. Sci. Eng.* 157, 482–506.

[38] www.20sim.com

[39] Rabbi, S.F., Sarker, M., Rideout, D.G., Butt, S.D.and Rahman, M.A. (2015). Analysis of a hysteresis IPM motor drive for electric submersible pumps in harsh Atlantic offshore environments. ASME In: Proceeding of the 34th *International Conference on Ocean, Offshore and Artic Engineering*, St. John's, Newfoundland, Canada from May 31-June 5.

[40] Karnoop, D. C., Margolis, D. L., & Rosenberg, R. C., (1999). *System Dynamics; Modeling and Simulation of Mechatronics Systems*, 3rd ed., John Wiley & Sons, Inc., New York.

[41] Rao, S.S. (1995). *Mechanical Vibrations*, 3rd ed., Addison-Wesley Publishing Company, New York.

[42] Sarker, M., Rideout, D.G. and Butt, S.D. (2012). Dynamic model of an oilwell drillstring with stick-slip and bit-bounce interaction. Presented at 10th *International Conference on Bond Graph Modeling and Simulation*, Genoa, Italy, July 8-11.

[43] Karnopp, D. (1985). Computer simulation of stick-slip friction in mechanical dynamic systems. *ASME J. Dyn. Syst., Meas. Cont.*, 107, 100-103.

[44] Margolis, D. (2005). Fixed causality slip-stick friction models for use in simulation of non-linear systems. *Journal of Systems and Control Engineering.*, 219, 199-206.

[45] Sarker, M., Rideout, D.G. and Butt, S.D. (2017). Dynamic model for longitudinal and torsional motions of a horizontal oilwell drillstring with wellbore stick-slip friction. *J. Petrol. Sci. Eng*., 150, 272-287.

[46] Sarker, M., Rideout, D.G. and Butt, S.D. (2017). Dynamic model for 3D motions of a horizontal oilwell BHA with wellbore stick-slip whirl interaction. *J. Petrol. Sci. Eng.*, 157, 482-506.

Appendix A

An overview of bond graph formalism

Bond graph is an explicit graphical tool for capturing the energetic structure of a physical system and uniquely suited to the understanding of physical system dynamics. Because of the ability to provide concise description of complex systems the bond graph formulation can be used in hydraulics, mechatronics, thermodynamic and electric systems. The bond graph language expresses a general class of physical systems through power (effort and flow) interactions and the factors of power have different interpretations in different physical domains.

Table A1 expresses the generalized power (effort and flow) variables and energy (momentum and displacement) variables in some physical domains. The generalized inertias and capacitance in bond graph **[40]** store energy as a function of the system state variables, the sources provide inputs from the environment, and the generalized resistors remove energy from the system. The state variables are generalized momentum and dis-placement for inertias and capacitances, respectively. Where the time derivatives of generalized momentum p and displacement q are generalized effort *e* and flow *f*. The power-conserving elements allow changes of state to take place. Such elements include power-continuous generalized transformer (TF) and gyrator (GY) elements that algebraically relate elements of the effort and flow vectors into and out of the element. In certain cases, such as large motion of rigid bodies in which coordinate transformations are functions of the geometric state, the constitutive laws of these power-conserving elements can be state modulated. Dynamic force equilibrium and velocity summations in rigid body systems are represented by power-conserving elements called 1 and 0 junctions, respectively.

Table A1: Generalized bond graph quantities

Variable	General	Translation	Rotation
Effort	$e(t)$	Force	Torque
Flow	$f(t)$	Velocity	Angular Velocity
Momentum	$p=\int e\,dt$	Linear momentum	Angular momentum
Displacement	$q=\int f\,dt$	Displacement	Angular displacement
Energy	$E(p)=\int^{p} f\,dp$ $E(q)=\int^{q} e\,dq$	Kinetic potential	Kinetic Potential

Table A2: Bond graph elements

	SYMBOL	CONSTITUTIVE LAW (LINEAR)	CAUSALITY CONSTRAINTS
SOURCES			
Flow	Sf ⟼	f = f(t)	fixed flow out
Effort	Se ⟶	e = e(t)	fixed effort out
ENERGETIC ELEMENTS			
Inertia	⟶ I ⟼ I	$f=\frac{1}{I}\int e\,dt$ $e=I\frac{df}{dt}$	preferred integral
Capacitor	⟼ C ⟶ C	$e=\frac{1}{C}\int f\,dt$ $f=C\frac{de}{dt}$	preferred integral
Resistor	⟼ R ⟶ R	$e=Rf$ $f=\frac{1}{R}e$	none

	SYMBOL	CONSTITUTIVE LAW (LINEAR)	CAUSALITY CONSTRAINTS
2-PORT ELEMENTS			
Transformer	1 ⟶ TF n ⟶ 2	$e_2 = n\,e_1$ $f_1 = n\,f_2$	effort in – effort out, or flow in – flow out
Modulated Transformer	θ ↓, 1 ⟶ MTF n(θ) ⟶ 2	$e_2 = n(\theta)\,e_1$ $f_1 = n(\theta)\,f_2$	
Gyrator	1 ⟼ GY n ⟶ 2	$e_2 = n\,f_1$ $e_1 = n\,f_2$	flow in – flow out, or effort in – effort out
Modulated Gyrator	θ ↓, 1 ⟼ MGY n(θ) ⟶ 2	$e_2 = n(\theta)\,f_1$ $e_1 = n(\theta)\,f_2$	
CONSTRAINT NODES			
1-junction	1 ⟶ 1 ⟶ 2, 1 ⟶ 3	$e_2 = e_1 - e_3$ $f_1 = f_2$ $f_3 = f_2$	one flow input

Appendix B

bond graph models

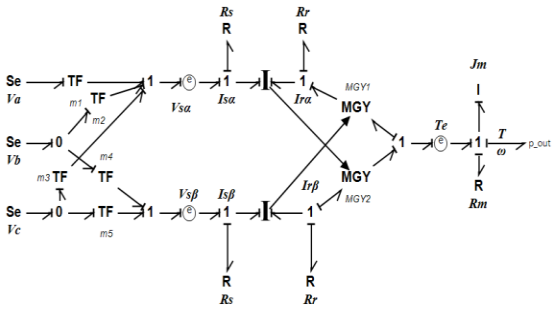

Figure B1: Bond graph model of an Induction motor

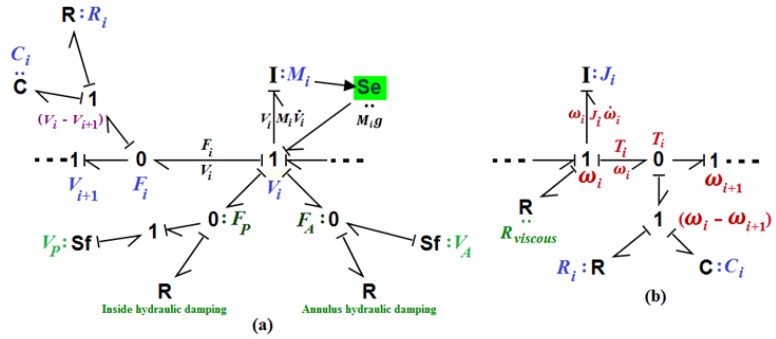

Figure B2: Bond graph segment model for (a) longitudinal (or axial) and (b) torsional motions of vertical section of drillstring.

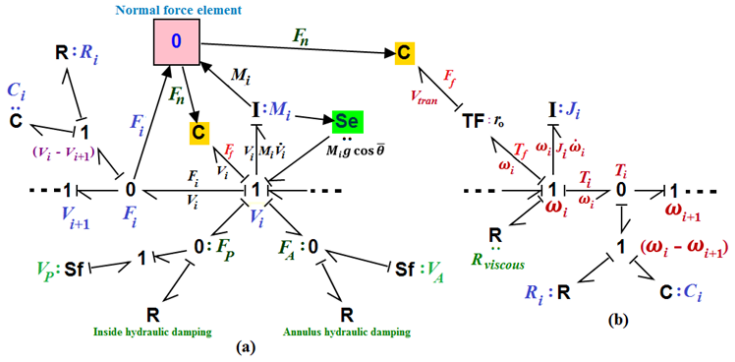

Figure B3: Bond graph segment model for (a) longitudinal (or axial) and (b) torsional motions of build (curved) section of drillstring.

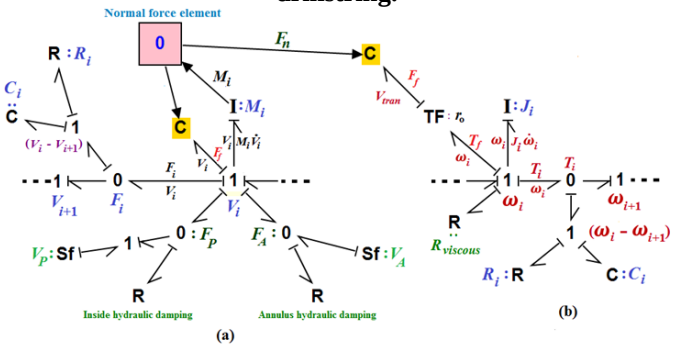

Figure B4: Bond graph segment model for (a) longitudinal (or axial) and (b) torsional motions of horizontal section of drillstring.

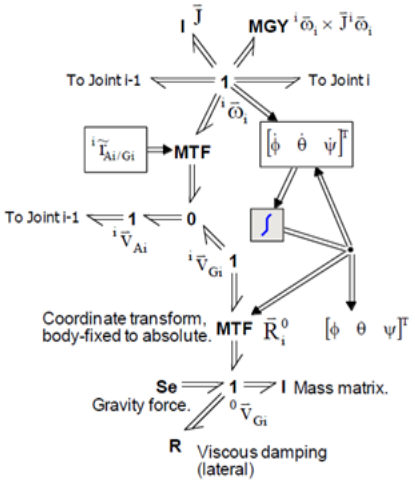

Figure B5: **Body i bond graph**

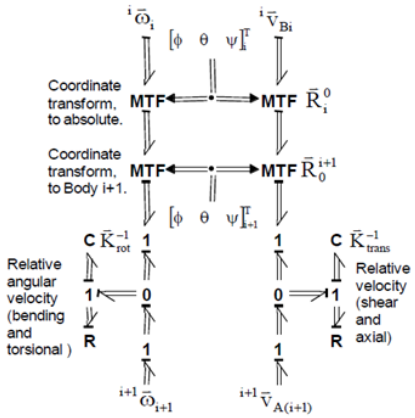

Figure B6: **Joint i bond graph**

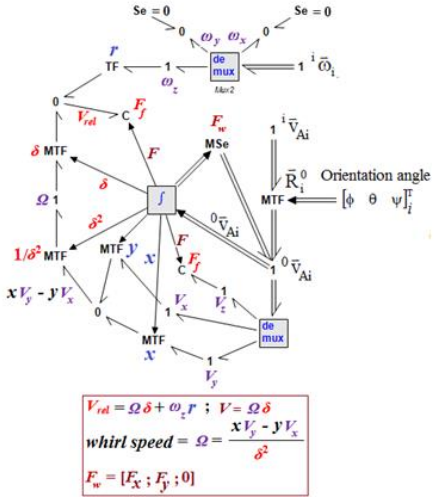

Figure B7: **Bond graph model for drillstring-wellbore contact and friction.**

Appendix C

Simulation data

Table C1.
Data used in horizontal oilwell drilling simulation

Parameters	values	Parameters	values
Drillstring data			
Swivel and derrick mass	7031 kg	Surface elevation amplitude s_0	0.001
Kelly length	15 m	Bit factor, b	1
Kelly outer diameter	0.379 m	Cutting coefficient ξ, C_1, C_2	1, 1.35×10^{-8}, -1.9×10^{-4}
Kelly inner diameter	0.0825 m	Frictional coefficient μ_0, α,β, γ, ν	0.06, 2, 1, 1, 0.01
DP outer diameter	0.101 m (4 in)	Threshold force, W_{fs}	10000 N
DP inner diameter	0.0848 m (3.34 in)	***Hydraulic data***	
SUB outer diameter	0.136 m (5.354 in)	Mud fluid density, ρ_m	1198 kg/m^3
SUB inner diameter	0.057 m (2.244 in)	Mud flow rate, Q	$Q_m + Q_a \sin(qt)$
collar outer diameter	0.125 m (4.921 in)	Mean mud flow rate, Q_m	0.022 m^3/s
collar inner diameter	0.060 m (2.362 in)	Mud flow pulsation amplitude, Q_a	0.002 m^3/s
motor HS outer diameter	0.121 m (4.763 in)	Freq. of variation in mud flowrate, q	25.13 rad/s
motor HS inner diameter	0.0 m (0.0 in)	Equivalent fluid viscosity for fluid resistance to rotation μ_e	30×10^{-3} Pa-s
Drillstring material	Steel	Weisbach friction factor outside drill pipe or collar, α_a	0.045
Wellbore diameter	0.18 m (7.086 in)	Weisbach friction factor inside drill pipe or collar, α_p	0.035
Drill bit-rock data		***Motor data***	
Bit type	PDC (Single cutter)	V, f, P	2300 V, 377 rad/s, 4 pole
Drill bit diameter	0.159 m (6.259 in)	L_{ls} & L_{lr}	0.0032 H, 0.0032 H
Drill bit mass	65 kg	L_m	0.14329 H
Bit type	PDC	R_s & R_r	0.262, 0.187
		J_m, R_m	11.06 kg.m^2, 0.05 Ω

Table C2.
Physical parameters of rock for simulation analysis

Rock type	Stiffness, k (N/m)	Damping, b (N.s/m)
Hackensack Siltstone	2.23×10^9	2.3×10^5
Pierre Shale I	6.93×10^7	3.89×10^4

Mejbahul Sarker
Lecturer, Department of Petroleum Engineering, American University of Kurdistan.